



**HAL**  
open science

# Reactive electrochemical membrane for the elimination of carbamazepine in secondary effluent from wastewater treatment plant

Oleksandra Ganzenko, Philippe Sizat, Clément Trelu, Valérie Bonniol, M. Rivallin, Marc Cretin

## ► To cite this version:

Oleksandra Ganzenko, Philippe Sizat, Clément Trelu, Valérie Bonniol, M. Rivallin, et al.. Reactive electrochemical membrane for the elimination of carbamazepine in secondary effluent from wastewater treatment plant. *Chemical Engineering Journal*, 2021, 419, pp.129467. 10.1016/j.cej.2021.129467 . hal-03647324

**HAL Id: hal-03647324**

<https://hal.umontpellier.fr/hal-03647324v1>

Submitted on 24 Apr 2023

**HAL** is a multi-disciplinary open access archive for the deposit and dissemination of scientific research documents, whether they are published or not. The documents may come from teaching and research institutions in France or abroad, or from public or private research centers.

L'archive ouverte pluridisciplinaire **HAL**, est destinée au dépôt et à la diffusion de documents scientifiques de niveau recherche, publiés ou non, émanant des établissements d'enseignement et de recherche français ou étrangers, des laboratoires publics ou privés.



Distributed under a Creative Commons Attribution - NonCommercial 4.0 International License

# Reactive electrochemical membrane for the elimination of carbamazepine in secondary effluent from wastewater treatment plant

Oleksandra Ganzenko<sup>a,b</sup>; Philippe Sizat<sup>a</sup>, Clément Trelu<sup>b</sup>; Valérie Bonniol<sup>a</sup>,  
Matthieu Rivallin<sup>a\*</sup>; Marc Cretin<sup>a\*</sup>

<sup>a</sup> Institut Européen des Membranes, IEM, UMR 5635, Univ Montpellier, CNRS, ENSCM, Montpellier, France

<sup>b</sup> Université Gustave Eiffel, Laboratoire Géomatériaux et Environnement, EA 4508, UPEM, 77454 Marne-la-Vallée, France

\*Corresponding authors

E-mail : marc.cretin@umontpellier.fr; [matthieu.rivallin@umontpellier.fr](mailto:matthieu.rivallin@umontpellier.fr)

Telephone: +33 (0)4 67 14 91 94; +33 (0)4 67 14 91 30

## Abstract

This study evaluated the feasibility of the electrooxidation process using a sub-stoichiometric titanium oxides ( $\text{TiO}_x$ ) reactive electrochemical membrane (REM) as anode for the treatment of a secondary effluent from a wastewater [treatment plant](#). The main objectives were to analyze (i) the degradation of a pharmaceutical pollutant, carbamazepine, added at a concentration of  $100 \mu\text{g L}^{-1}$ , (ii) the mineralization of the residual total organic carbon ( $\text{TOC} = 7 \text{ mg L}^{-1}$ ), (iii) the formation of toxic by-products and (iv) the energy consumption of the REM process. Two main operating parameters were tested: the current density applied to the REM ( $74, 149$  and  $290 \text{ A m}^{-2}$ ) and the flux of TOC passing through the membrane. The results revealed that the efficiency of the process was maintained above 70% of mineralization and >98% of degradation of carbamazepine until a limiting value of TOC flux was reached. The higher the current density, the higher the limiting value of the TOC flux above which the efficiency decreased. This trend was ascribed to the limitation from the amount of reactive species produced on the REM surface (current limitation instead of mass transport limitation at lower TOC flux). As the energy efficiency strongly increased when applying a higher TOC flux, it is therefore crucial to apply the process around this threshold value. This study also showed that it is possible to control the formation of toxic chlorine-containing by-products ( $\text{ClO}_3^-$ ,  $\text{ClO}_4^-$ ,  $\text{AOCl}$ ) by decreasing the current density. This issue is particularly important for such effluents containing a significant amount of  $\text{Cl}^-$  ions. By taking into consideration both advantages and drawbacks, optimal results were obtained with the lowest current density of  $73 \text{ A m}^{-2}$  and a TOC flux through the membrane of  $4.41 \text{ g h}^{-1} \text{ m}^{-2}$  corresponding to  $1.34 \text{ m}^3 \text{ h}^{-1} \text{ m}^{-2}$ . These conditions allowed for >98% degradation of carbamazepine and 70% of mineralization with an energy consumption of  $0.15 \text{ kWh g}^{-1}$  of TOC removed (i.e.  $0.74 \text{ kWh m}^{-3}$  of treated wastewater).

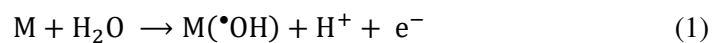
## Keywords

Reactive electrochemical membrane, sub-stoichiometric titanium oxide, anodic oxidation, secondary effluent, carbamazepine.

## 1. Introduction

Membrane filtration processes are widely applied in modern wastewater treatment plants (WWTP) all over the world. Electrochemical methods for water treatment are emerging technologies showing a promising perspective and inciting great scientific interest. Membrane processes have two major drawbacks. First, it is only a separation process, where pollutants are concentrated in the retentate. Then, nanofiltration membranes with low pore size used for the retention of micropollutants require the use of high transmembrane pressure. Besides, large-scale application of electrochemical processes for the removal of micropollutants is strongly affected by mass transport limitations when treating low concentration of pollutants, which leads to a low energy efficiency. However, the combination of these two processes aims at being a synergetic technology enhancing the advantages of both processes. The idea is based on coupling both processes for the removal of pollutants passing through a reactive electrochemical membrane used as anode for the anodic oxidation process.

Anodic oxidation is an electrochemical advanced oxidation process allowing the removal of organic pollutants through different mechanisms including (i) direct electron transfer and (ii) mediated oxidation by generation of reactive radical species [1-3]. Particularly, the generation of strong oxidant species is possible when using anode materials with high overvoltage for oxygen evolution reaction [4-8]. In this case, hydroxyl radicals can be produced from the one-electron oxidation of water at the electrode surface M (Eq. 1). Hydroxyl radicals present a major advantage of being a non-selective and highly oxidizing agent.



In order to improve process efficiency, it is necessary to improve the amount of organic pollutants available for reaction with oxidant species at the anode surface where most of oxidation reactions take place. By using dense plate electrodes, the mass transport of pollutants from the bulk solution to the anode surface is strongly limited by the diffusion boundary layer close to the material surface. This limitation can be addressed by using REM with low pore size and high electrochemically active

surface as detailed in mechanistic studies dedicated to flow-through electrochemical technologies [9, 10, 11, 12]. REM strongly decreases the diffusion time of organic compounds from the center of a pore to the electrode surface and consequently mass transport can be strongly improved by increasing the convection through the REM. Therefore, the flux of organic compounds passing through the REM becomes a crucial operating parameter [13, 14, 15].

However, a great challenge remains the synthesis of suitable materials that can be used as REM. REM must provide (i) a sufficient conductivity, (ii) a high overvoltage for oxygen evolution reaction and (iii) a suitable porosity for membrane filtration and enhanced mass transport conditions (in the micro- or nanometer range). In this context sub-stoichiometric titanium oxide ( $\text{TiO}_x$ ) is a promising ceramic material, which presents critical advantages from both cost and operational aspects with a well-established production technology and an acceptable price tag. Among  $\text{TiO}_x$  phases,  $\text{TiO}_{1.75}$  (*i.e.*  $\text{Ti}_4\text{O}_7$ ) has the highest conductivity (around  $1000 \text{ S cm}^{-1}$ ) and is robust from mechanical, chemical and thermal standpoints [16]. It can be produced from  $\text{TiO}_2$  reduction by Ti metal as a powder [17] or pressed pellets [18] or by reduction under nitrogen [19] or hydrogen [20] gas flux. The combination of a sol-gel synthesis with spark plasma sintering or vacuum-carbothermic process was also reported for synthesis of nanostructured  $\text{Ti}_4\text{O}_7$  materials for applications in thermoelectricity [21] or supercapacitor and electrocatalysis [22]. In 2016, it was also reported the possibility to synthesize porous  $\text{Ti}_4\text{O}_7$  from tubular asymmetric  $\text{TiO}_2$  ultrafiltration membranes for their further used as REM in water treatment, focusing on both kinetic and thermodynamic aspects [23]. Probe molecules have been used in order to highlight the hydroxyl radical mediated oxidation as well as the convection-enhanced mass transport of organic compounds [24]. Model compounds have also been used for investigating the production of chlorinated by-products [25]. Density functional theory calculations have been coupled with experimental approaches in synthetic solutions in order to better understand reactions with organic compounds at the REM interface [26].

$\text{Ti}_4\text{O}_7$  REM anode has then proved its high energy-efficiency for electrochemical oxidation of highly stable perfluoroalkyl substances in synthetic solutions [27].  $\text{Ti}_4\text{O}_7$  REM anode was also coupled with the cathodic electro-Fenton process in a flow-through pilot to treat paracetamol as a model pollutant.

It was emphasized a synergistic effect related to the formation of carboxylic acids from paracetamol degradation in the bulk retentate that are more easily mineralized at the REM where both OH-mediated oxidation and direct electron transfer occur [28]. However, as regards to real effluents, only dense plate  $\text{Ti}_4\text{O}_7$  was successfully used for mineralization and biodegradability enhancement of nanofiltration concentrate of landfill leachates [29]. Therefore, further application and development of this material now depends on feasibility studies related to (i) the application of these REM for the treatment of real effluents containing low concentration of biorefractory pollutants, (ii) the assessment of energy consumption and (iii) the evaluation of the formation of toxic by-products.

In this study, the feasibility of implementing  $\text{Ti}_4\text{O}_7$  REM in a flow-through reactor for the treatment of a WWTP secondary effluent was assessed in terms of (i) mineralization of the organic matter (ii) degradation of a micropollutant, carbamazepine (CBZ), added at  $100 \mu\text{g L}^{-1}$  (iii) production of toxic chlorine-containing by-products and (iv) energy consumption. The process efficiency was assessed in dependence of the two main operating parameters, which are the current density and the permeate flux. The objective was to understand and to identify the key parameters for minimizing the energy consumption, optimizing the removal effectiveness and reducing the formation of toxic by-products. Thus, this study investigates for the first time the suitability of using  $\text{Ti}_4\text{O}_7$  REM for the treatment of a real WWTP secondary effluent polluted with a low concentration of pharmaceuticals.

## **2. Materials and methods**

### *2.1. Secondary effluent*

The pilot reactor was fed with a secondary effluent sampled from a WWTP located in La Grande Motte in the south of France. The WWTP is equipped with a Kubota® Submerged membrane unit (SMU RW 400). The nominal pore size of the membrane sheet is  $0.2 \mu\text{m}$ . All samples have been collected at stationary phase (stable operating parameters and stable removal efficiencies of the systems) and the main characteristics of the effluent are presented in Table 1. The effluent was doped with  $100 \mu\text{g L}^{-1}$  of CBZ.

**Table 1.** Main characteristics of the secondary effluent.

Parameter	Value	Parameter	Value mg.L <sup>-1</sup>
COD	24.2 ± 2.7 mgO <sub>2</sub> L <sup>-1</sup>	[NO <sub>2</sub> <sup>-</sup> ]	0.3 ± 0.1
TOC	7 mg C L <sup>-1</sup>	[NO <sub>3</sub> <sup>-</sup> ]	13.8 ± 1.9
Conductivity	2.5 ± 0.3 mS cm <sup>-1</sup>	[SO <sub>4</sub> <sup>2-</sup> ]	229 ± 4
pH	7.2 – 7.8	[Br <sup>-</sup> ]	1.5 ± 0.2
Abs 254 nm	0.128 – 0.157	[Cl <sup>-</sup> ]	556 ± 65
[PO <sub>4</sub> <sup>3-</sup> ]/[NH <sub>4</sub> <sup>+</sup> ]	not detected	[ClO <sub>3</sub> <sup>-</sup> ]	1.4 ± 0.2

## 2.2. Chemicals

All chemicals used in this study were of reagent grade, purchased from Sigma Aldrich, including CBZ (CAS 298-46-4), sodium sulfate (CAS 7757-82-6), acetonitrile and formic acid. Ultrapure water was obtained from a Milli-Q system (Millipore Co. Ltd, resistivity > 18.2 MΩ cm).

## 2.3. Experimental pilot reactor

The experimental lab pilot was made of a 3 L feed tank, a pump for circulation of the feed solution, a recirculation loop for the retentate, a DC power supply (from ELC, model AL924A) and a homemade electrochemical membrane cell (Fig. 1). The retentate was continuously recirculated and the permeate was collected for analysis.

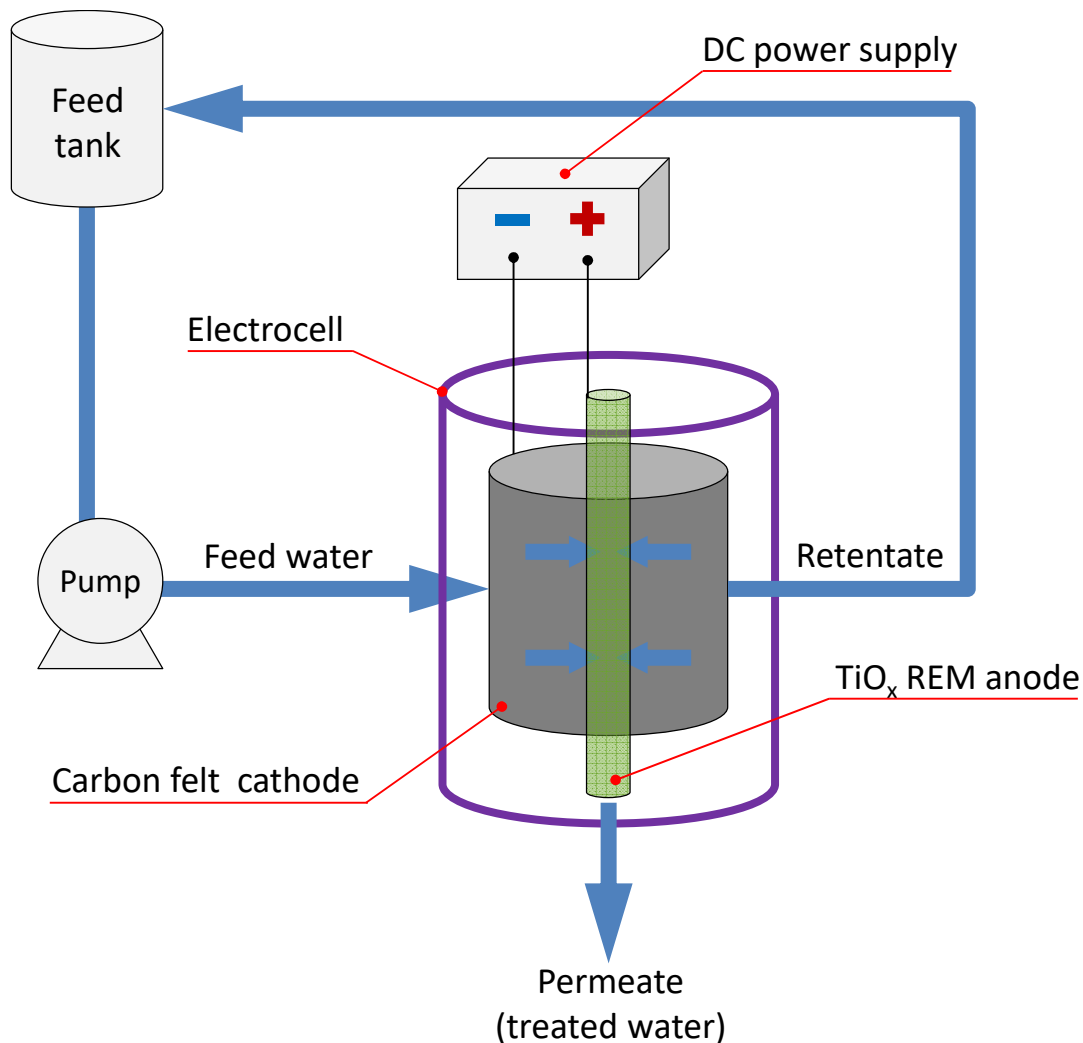


**Fig. 1.** Scheme of the pilot equipped with a  $\text{Ti}_4\text{O}_7$  reactive electrochemical membrane (REM in green in the center) for electro-oxidation of secondary effluents doped with CBZ at  $100 \mu\text{g L}^{-1}$

The whole setup was developed at European Membrane Institute of Montpellier. The  $\text{Ti}_4\text{O}_7$  REM anode had the following dimensions: active length of 9 cm, inner diameter of 6 mm, outer diameter of 10 mm, and was used in outside-inside cross-flow filtration mode. The REM was developed and obtained from Saint Gobain CREE. Detailed characterization of this material was given in Trellu *et al.* [14, 28]. The anode is a mixture of  $\text{Ti}_4\text{O}_7$  and  $\text{Ti}_5\text{O}_9$  Magnéli phases. It presents a monodispersed pore size distribution, with a median pore size of  $1.4 \mu\text{m}$ , a porosity (pore volume) of 41% and a specific surface area of  $0.40 \text{ m}^2 \text{ g}^{-1}$ . The water permeability of the membrane is  $3300 \text{ L m}^{-2} \text{ h}^{-1} \text{ bar}^{-1}$ .

Scanning electron microscopy images, Hg intrusion porosimetry and X-ray diffraction data are



provided as Supplementary Material. The cathode is a 3 mm thick carbon felt encircling the inner wall of the electrochemical cell with an interelectrode distance of 3 cm with the REM. Experiments were performed at the natural pH of the effluent ( $7.5 \pm 0.3$ ). Experiments were conducted in galvanostatic mode with a current density of 73, 145 and 290 A m<sup>-2</sup> according to the external geometric surface area of the REM. The feed compartment was maintained under a nitrogen flux in order to avoid H<sub>2</sub>O<sub>2</sub> production at the carbon felt under cathodic polarization.

#### *2.4. Total Organic Carbon (TOC) analysis*

Total organic carbon was measured using a Shimadzu TOC-L analyzer (680 °C catalytic combustion method). The relative standard deviation on TOC measurement was 2%. Calibration was performed using several dilutions of a standard from Accu SPEC (1000 µg C mL<sup>-1</sup>).

#### *2.5. Ions analysis*

Anions and cations were analyzed by ion chromatography. Anions (Cl<sup>-</sup>, NO<sub>2</sub><sup>-</sup>, ClO<sub>3</sub><sup>-</sup>, NO<sub>3</sub><sup>-</sup>, SO<sub>4</sub><sup>2-</sup>, PO<sub>4</sub><sup>3-</sup>, Br<sup>-</sup>) were followed using a chromatographic system Dionex Thermofisher ICS1000 with an eluent producer, equipped with a Dionex Thermofisher AS19 column, an ARDS 600 suppressor and a conductivity detector. The eluent was an aqueous solution of potassium hydroxide. Gradient elution was used in the following manner: 10 mM during the first 10 min, then increase up to 45 mM during 20 min and finally 10 mM during the last 10 min of analysis. The flow was fixed at 1 mL min<sup>-1</sup>.

The analysis of cations (Na<sup>+</sup>, NH<sub>4</sub><sup>+</sup>, K<sup>+</sup>, Mg<sup>2+</sup>, Ca<sup>2+</sup>) was performed by a chromatographic system Dionex Thermofisher ICS900, equipped with a Dionex Thermofisher CS12A column, a CERS 500 suppressor and a conductivity detector. A solution of 20 mM methanesulfonic acid was used as eluent in isocratic mode at 1 mL min<sup>-1</sup>.

#### *2.6. Monitoring of carbamazepine degradation*

The degradation of CBZ was followed by high performance liquid chromatography (HPLC) coupled with mass spectrometry (MS). The HPLC system (Waters Alliance 2695 HPLC Pump and Waters

Alliance 2695 Autosampler) was equipped with a C18 column (L = 50 mm, D = 2 mm, particle size = 5 $\mu$ m) thermostated at 20°C. The detector was a triple quadrupole mass spectrometer (Quattro Micro API by Waters). Injection volume was 5  $\mu$ L. The composition of the mobile phase was 75% milliQ water and 25% acetonitrile with 0.1% (v/v) formic acid eluted in isocratic mode at 0.250 mL min<sup>-1</sup>. The duration of analysis was 3 min and the elution time of CBZ was 1.71 min. The calibration curve for quantification of CBZ concentration was performed with the real effluent doped with 100  $\mu$ g L<sup>-1</sup> of CBZ in order to minimize the effect of the matrix noise on the analysis. The detection limit was found to be 2  $\mu$ g L<sup>-1</sup>.

The triple quadrupole MS was operated in multiple reaction monitoring with compounds being ionized in the positive electrospray ionization mode (MRM: 237.2  $\rightarrow$  194.2 with MH<sup>+</sup> = 237.2, fragment Q1 = 194.2). The detection conditions were: capillary potential of 3.5 kV, cone potential of 25V, collision energy of 20V, source temperature of 120°C, desolvation temperature of 450°C, cone gas flow of 50 L h<sup>-1</sup>, desolvation gas flow of 450 L h<sup>-1</sup>. Nitrogen was used as nebulizer gas.

### *2.7. Analysis of halogen-specific adsorbable organic halogen (AOX)*

Prior to the analysis, the residual free chlorine was measured by the diethyl-p-phenylenediamine (DPD) method and each sample was quenched with Na<sub>2</sub>SO<sub>3</sub> aqueous solution in proportion 1.2 mol for 1 mol of residual chlorine. Then, 1 mL of nitrate stock solution ([NaNO<sub>3</sub>] = 0.2 mol L<sup>-1</sup>, containing 25 mL L<sup>-1</sup> HNO<sub>3</sub> 65%) was then added according to the ISO 9562 method. Then, the samples were passed through the carbon columns (containing activated carbon (AC) with a grain size distribution around 50-150  $\mu$ m, provided by Envirosciences). Then, 10 mL of a nitrate solution was passed in order to remove any inorganic species. A blank sample was also prepared in the same way, using Milli-Q water. The activated carbon columns containing the adsorbed organic halogens were transferred to ceramic boats for combustion using a Mitsubishi AQF-2100H unit. The hydrogen halide gases produced were collected in ultra pure water contained in an absorption tube of the gas absorption unit (Mitsubishi GA-210).

The solution in the absorption tube was then analyzed on-line for chloride, bromide, and iodide using ion chromatography (Thermo Scientific Dionex Integrion HPIC system). The concentrations of

chloride, bromide, and iodide obtained from the ion chromatograph analysis corresponded to the concentrations of adsorbable organic chloride (AOCl), bromide (AOBr), and iodide (AOI), respectively.

### 2.8. Energy consumption

Energy consumption (EC) was expressed as either kWh per g of TOC removed (Eq. 2) or kWh per m<sup>3</sup> of treated water (Eq. 3).

$$EC(Wh (g TOC)^{-1}) = \frac{E_{cell} * I}{(TOC_f - TOC_p) * Q} \quad (1)$$

$$EC(Wh m^{-3}) = \frac{E_{cell} * I}{Q} \quad (2)$$

Where  $E_{cell}$  is the average cell voltage (V),  $I$  the applied current (A),  $Q$  is the permeate flow (m<sup>3</sup> h<sup>-1</sup>), and  $TOC_f$  and  $TOC_p$  are the experimental TOC concentrations (g C m<sup>-3</sup>) at a given time in the feed and the permeate, respectively.

## 3. Result and discussion

### 3.1. Mineralization of the secondary effluent doped with carbamazepine

Control experiments were previously performed on those membranes [14]. Results obtained without current supply showed the absence of adsorption and retention of dissolved organic compounds. The main reasons are that (i) the specific surface area of 0.40 m<sup>2</sup> g<sup>-1</sup> is low compared to materials tailored for adsorption and (ii) the mono-modal pore size distribution ranging between 0.8 and 1.9 μm with median pore diameter of 1.4 μm does not allow any retention of dissolved compounds

Mineralization of the effluent was followed for three different current densities (73, 145 and 290 A m<sup>-2</sup>). Different transmembrane pressures were tested for each applied current density, which resulted in the variation of the permeate flux. Electrochemical processes for the treatment of low concentrations of pollutants are usually operated under mass transport limitation, meaning that they are limited by the

transport of organic compounds from the bulk to the electrode surface. Therefore, this study selected as crucial parameter the amount of organic matter that passed through the membrane (TOC flux) instead of the volumetric permeate flux. The TOC flux is the product of the initial value of TOC in the effluent and the volumetric permeate flux. The TOC flux elimination was defined similarly, by taking into consideration the amount of TOC removed by the process. Therefore, results are presented in fig. 2 as TOC flux elimination versus the TOC flux through the REM.

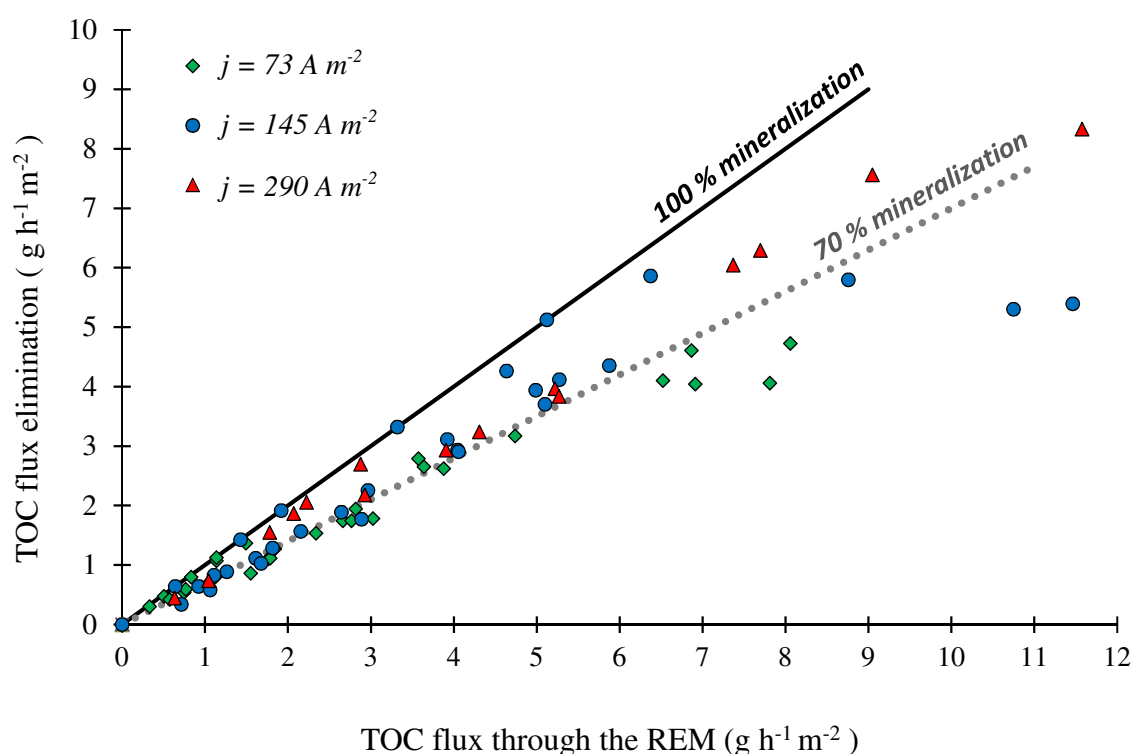


**Fig. 2.** Mineralization of the real effluent doped with  $100 \mu\text{g L}^{-1}$  of CBZ in dependence on applied current density and TOC flux through the reactive electrochemical membrane.

As can be seen from fig. 2, for all current densities, mineralization can be maintained between 70 and >98% up to a maximum value of TOC flux. Then, at higher TOC flux, a plateau is observed for the TOC flux elimination (it corresponds to a drop of the percent removal of TOC). This maximum value of TOC flux strongly depends on the applied current density. The value of TOC flux at which the drop in efficacy occurred was between 5 and  $6 \text{ g h}^{-1} \text{ m}^{-2}$  for the lowest current density, while for the middle value it was around  $8 - 9 \text{ g h}^{-1} \text{ m}^{-2}$ . For the highest current density of  $290 \text{ A m}^{-2}$ , this plateau is

projected to be reached at values of TOC flux higher than  $12 \text{ g h}^{-1} \text{ m}^{-2}$ . In this way, it was clear that the higher the current density applied, the higher the limiting flux was. This could be explained by taking into consideration both mass transport and current limitations. The use of REM instead of conventional plate electrodes has the major goal of reducing the mass transport limitation. In fact, owing to the low pore size of the REM, the diffusion characteristic time of organic compounds from the center of a pore to the electrode surface is strongly decreased compared to the diffusion characteristic time of organic compounds through the diffusion layer at the surface of dense electrodes [15]. Therefore, it is possible to increase the mass transport of organic compounds at the surface of the REM simply by increasing convection, *i.e.* by increasing the permeate flux of the wastewater passing through the membrane. However, this study highlights that there is a limiting permeate flux above which the REM becomes mainly operated under current limitation instead of mass transport limitation. It means that above this threshold value, the amount of reactive species generated on the anode is not sufficient for the removal of the high TOC flux through the membrane. This current limitation is also consistent with the fact that the limiting value of the TOC flux is higher when the current intensity increases. In fact, a larger amount of organic compounds can be oxidized when increasing the amount of reactive species generated at higher current density.

### *3.2. Degradation of carbamazepine in the secondary effluent*

The degradation of an individual micropollutant is also an important parameter in order to study the capacity of the process to maintain a high degradation rate of target pollutants. The results are presented on fig. 3 giving the normalized concentration of CBZ in the permeate as a function of TOC flux through the REM. At the lowest values of TOC flux, CBZ was not detected in the permeate (CBZ degradation above 98% because the detection limit of CBZ was found to be  $2 \mu\text{g L}^{-1}$ ). A similar behavior was observed for the evolution of the percent of degradation of CBZ and mineralization of TOC. CBZ was fully degraded after passing through the REM only until a limiting value of TOC flux was reached. This value depends on the current density applied. For the lowest current density of  $73 \text{ A m}^{-2}$ , CBZ started to be detected in the permeate at the value of  $4 - 5 \text{ g h}^{-1} \text{ m}^{-2}$ . For the middle value of

current density of  $145 \text{ A m}^{-2}$ , this value was twice as high as for the lowest, around  $8 - 9 \text{ g h}^{-1} \text{ m}^{-2}$ , while for the highest current density, this limiting TOC flux was around  $15 - 18 \text{ g h}^{-1} \text{ m}^{-2}$ . As explained in the previous section, this phenomenon of the threshold value can be explained by the operation of the process under current limitation when the TOC flux through the membrane becomes too high. It would be necessary to increase the applied current density in order keep a high value of degradation and mineralization rate of the process when the TOC flux exceeds this threshold value.

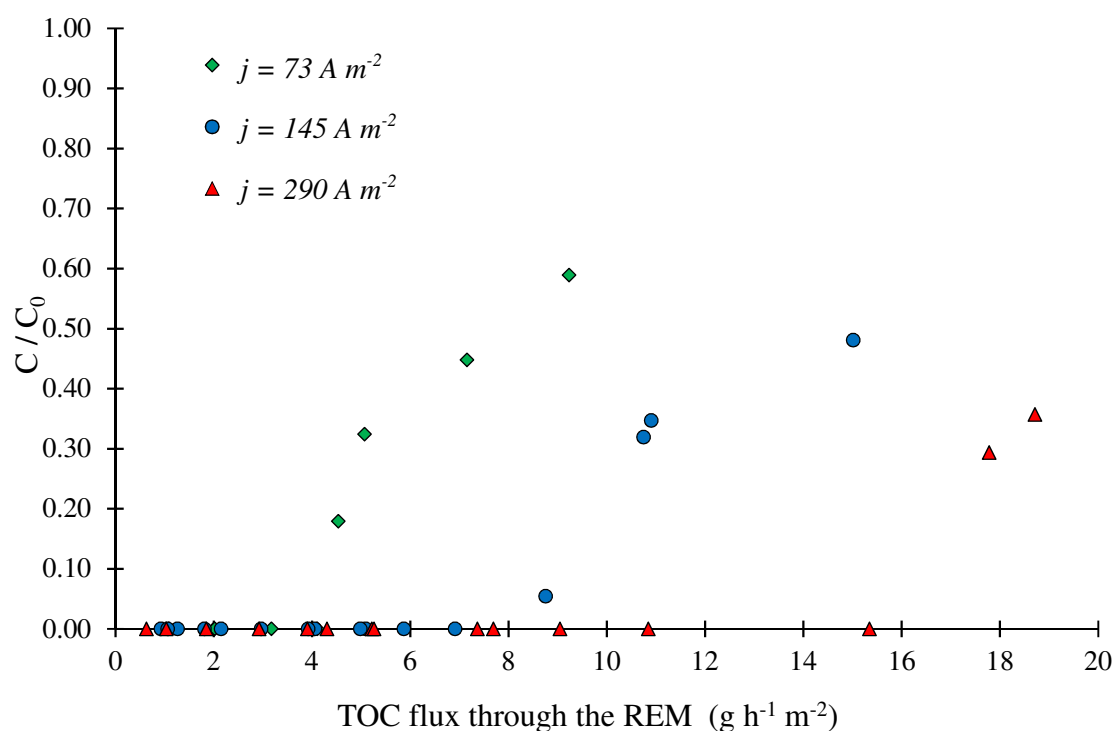


**Fig. 3.** Degradation of  $100 \mu\text{g L}^{-1}$  carbamazepine in the effluent in dependence of the TOC flux through the reactive membrane and the applied current density

Interestingly, the values of limiting flux for degradation and mineralization were similar. For example, for the middle current density, the limiting value of TOC flux for keeping TOC removal above 70% or for achieving >95% degradation of CBZ was in both case around  $8 - 9 \text{ g h}^{-1} \text{ m}^{-2}$ . Such conformity in results concerning the mineralization of the total organic pollution and degradation of CBZ supports the explanation by the change in process limitations as detailed above. Moreover, it is consistent with data reported in the literature on the anodic oxidation process. When AO is operated in batch reactor,

mineralization kinetics are often only slightly slower than degradation kinetics. In fact, anodic oxidation is a heterogeneous process during which oxidant species are accumulated at the surface of the electrode material. Thus, organic pollutants reaching the electrode surface can be rapidly mineralized by this high local concentration of oxidant species instead of being only degraded. This phenomenon represents a great advantage for the application of this process since the formation of potentially toxic degradation by-products can be therefore strongly reduced.

However, the degradation and mineralization of residual organic pollutants is not the only parameter to take into consideration for the evaluation of the suitability of this process. The feasibility of the application of a new water treatment process must also take into consideration the potential formation of various toxic by-products. Particularly, it was reported in the literature [2, 30] that two main drawbacks of anodic oxidation are (i) the generation of organo-halogenated compounds and (ii) the formation of chlorates and most importantly perchlorates. As the effluent released by the wastewater treatment plant contained more than  $550 \text{ mg L}^{-1}$  of chlorides, it was crucial to follow the evolution of these parameters. One of the main goals of the application of the electrochemical treatment methods to such effluents would also be the minimization of the formation of these problematic substances [30, 31].

### *3.3. Evolution of chlorates and perchlorates during the treatment*

The evolution of chlorides, chlorates and perchlorates is presented on fig. 4 in dependence of the applied current density. From the general A view of fig. 4, it is clear that chloride was oxidized in the process since its concentration in the permeate became lower than in the feed water. The B view from the same experiments (magnified view of A) gives a better visibility of the evolution of chlorates and perchlorates. All chloride removed from the solution was not transformed into chlorate and perchlorate since a large amount of chloride can also be transformed into volatile forms ( $\text{Cl}_2$ ,  $\text{ClO}_2$ ,  $\text{Cl}_2\text{O}$ ) and  $\text{HOCl}/\text{ClO}^-$  (which might be used for disinfection). For example, chlorate and perchlorate represented only 10, 14 and 43% of the total loss of chloride for experiments at 73, 145 and  $290 \text{ A m}^{-2}$ , respectively.

Concentration of chlorate in the permeate was in the range 15 – 50 mg L<sup>-1</sup> depending on the applied current density. Interestingly, the increase in chlorate concentration was proportional to the increase of the current density. It means that the formation of chlorate was depending on the electric charge (A h) without threshold effect related to the current density.

Perchlorate was also detected in the permeate. For example, a concentration of 25 mg L<sup>-1</sup> was observed at the highest current density. Perchlorate formation is a major drawback of anodic oxidation using anode materials with high overvoltage for oxygen evolution reaction. For example, Bergmann *et al.* [32] reported the formation of 123 mg L<sup>-1</sup> of perchlorate using boron-doped diamond (BDD) anode at 200 A m<sup>-2</sup> and 1.0 A h L<sup>-1</sup>. Therefore, it is not surprising to observe perchlorate in our case since the electric charge was 0.54 A h L<sup>-1</sup> for  $j = 290 \text{ A m}^{-2}$  and  $J = 540 \text{ L h}^{-1} \text{ m}^{-2}$ . However, on the contrary to chlorate, the concentration of perchlorate increased drastically by increasing the applied current density. The concentration was multiplied by 11 between 73 and 145 A m<sup>-2</sup> and by 17 between 145 and 290 A m<sup>-2</sup>. In this case, a threshold effect related to the current density was clearly observed. These results are consistent with the results reported in synthetic solutions treated with BDD by Sánchez-Carretero *et al.* [33]. In fact, a linear relation was reported between the electrical charge (with similar current density) and the formation of chlorate and perchlorate. However, the increase of the current density (with similar electrical charge) only increased the concentration of perchlorate. This might be ascribed to the complex mechanism of perchlorate formation involving both direct electron transfer and hydroxyl radical mediated oxidation, which is favored at high current density. Perchlorate formation was also reported to be strongly dependent on competitive ions and organic compounds. It has been reported that the formation of perchlorate might be strongly hindered when operating the process under current limitation in presence of organic compounds with high reaction rates with hydroxyl radicals [34]. This hydroxyl radical scavenging effect avoids the reaction of chlorates with hydroxyl radicals for the formation of perchlorates. This explanation might also be suitable for explaining the results observed in this study. In fact, results reported in fig. 4 have been obtained for experiments performed at a constant TOC flux of 3.8 g h<sup>-1</sup> m<sup>-2</sup>. Using low current density, this TOC flux is close to the limiting value corresponding to the operation of the process under current limitation, as observed in previous sections. For the higher current densities, this TOC flux is clearly



below this threshold value and the process is clearly operated under mass transport limitation, which favors the reaction of hydroxyl radicals with chlorates for the formation of perchlorates. The results reported in this study on a real effluent are crucial for assessing the potential of application of REM. In fact, they highlight that REM should be operated at low current density and under current limitation in order to avoid perchlorate formation. At flux of  $3.8 \text{ g h}^{-1} \text{ m}^{-2}$ , the perchlorate concentration was  $130 \mu\text{g L}^{-1}$  and  $1.46 \text{ mg L}^{-1}$  at  $73$  and  $149 \text{ A m}^{-2}$ , which was low considering the high chloride concentration of the initial effluent ( $556 \pm 65 \text{ mg L}^{-1}$ ). It was also noticed that the increase of nitrate concentration with the applied current density was definitely linked to mineralization of organic nitrogen.

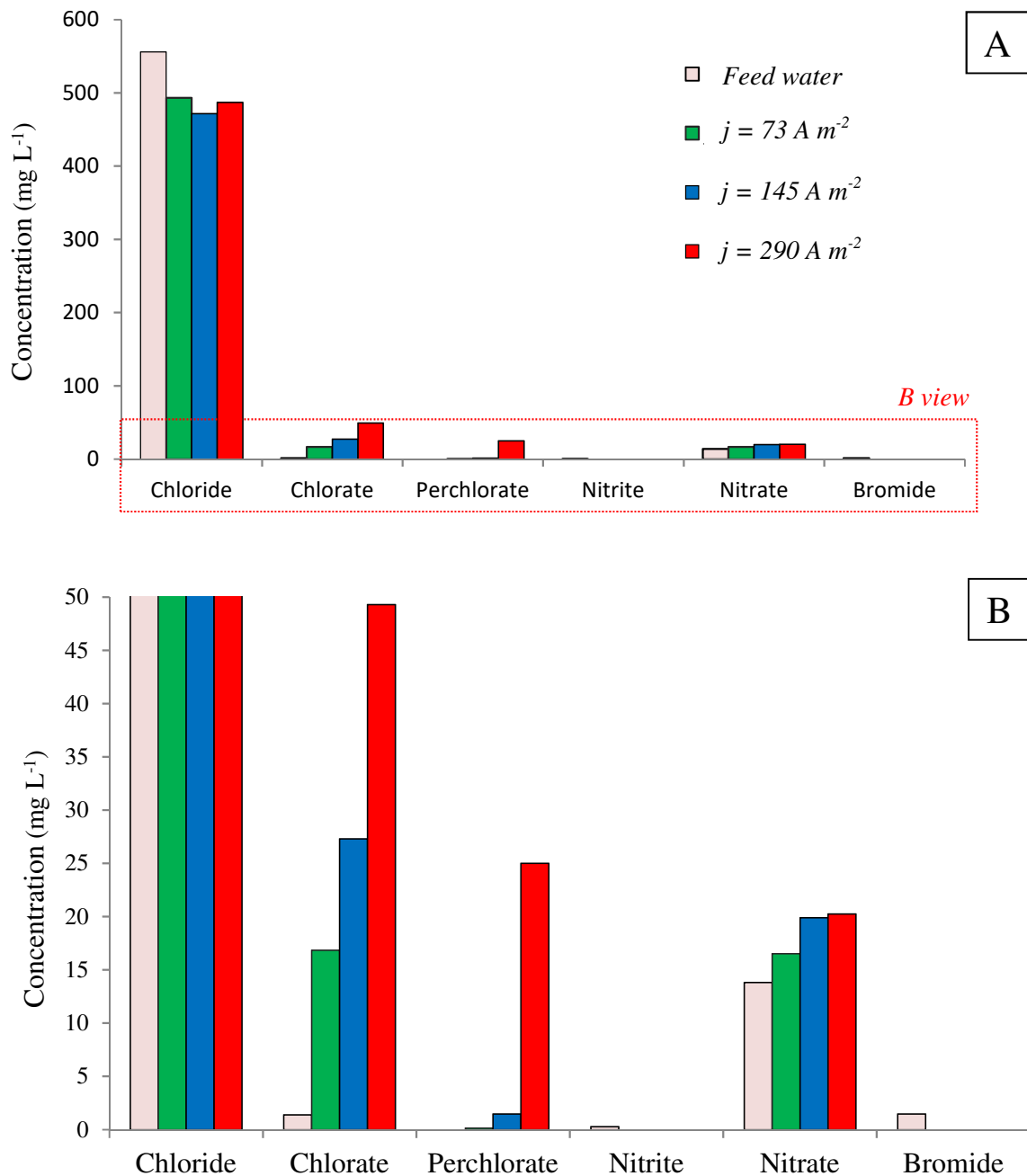


**Fig. 4.** Evolution of anions (perchlorates, chlorides, nitrates, bromides, chlorates, nitrates and sulfates) in dependence on the applied current density for a TOC flux of  $3.8 \text{ g h}^{-1} \text{ m}^{-2}$ .

A. General view B. Magnified view with a smaller scale on the y axis.

### 3.3. Evolution of adsorbable organo-halogenated compounds during the treatment

Apart from the chlorine-containing ions, the active chlorine available in the solution can react with the organics for forming the so-called organo-halogenated compounds, which are most of the time monitored through the amount of adsorbable organo-halogenated compounds (AOX). AOX are

generally considered as unwanted compounds with potential genotoxic effects [35-37]. The analyses showed the initial presence of these compounds at low concentration in the feed water (Table 2) under the form of organochloride compound (AOCl). The results obtained for AOBr and AOI were below the limit of detection ( $0.5 \mu\text{g L}^{-1}$ ) in all the samples.

**Table 2.** Concentration of adsorbable organic chlorides (AOCl) in initial effluent and in the treated samples in dependence on the applied current density for experiments performed at a constant TOC flux of  $3.8 \text{ g h}^{-1} \text{ m}^{-2}$ .

Samples	AOCl ( $\mu\text{g L}^{-1}$ )
Initial effluent	77.8
Effluent treated ( $j = 73 \text{ A m}^{-2}$ )	1491
Effluent treated ( $j = 290 \text{ A m}^{-2}$ )	4270

Three samples of treated water at two different current densities were also analyzed. A significant increase in the concentration of AOCl was observed for all samples. For the lowest current density the concentration of AOCl was around  $1.5 \text{ mg L}^{-1}$ , though for the highest current it increased to a value almost three times higher. The formation of these compounds often comes from reactions between free chlorine ( $\text{HOCl}/\text{ClO}^-$ ) and dissolved organic compounds through various possible pathways such as oxidation, addition or electrophilic substitution. By increasing current density with a factor 3.9, the AOCl formation was multiplied by 3.0. These results are consistent with literature since it was reported that the formation of AOCl is tightly correlated with the electric charge without threshold effect related to the current density [38]. In a previous study on the tertiary treatment of wastewater (with similar TOC of  $9.7 \text{ mg L}^{-1}$ ) with a BDD anode, an electric charge of  $0.13 \text{ A h L}^{-1}$  resulted in the formation of  $400 \mu\text{g L}^{-1}$ , while in this study  $1413 \mu\text{g L}^{-1}$  was formed after passing the same electric charge (for  $j = 73 \text{ A m}^{-2}$  and  $J = 540 \text{ L h}^{-2} \text{ m}^{-2}$ ) [38]. This higher value might be explained either by the higher chloride concentration ( $144 \text{ vs } 500 \text{ mg L}^{-1}$ ) or by the different electrode material used (further studies are required on the understanding of AOX formation with  $\text{Ti}_4\text{O}_7$  REM). The results obtained in the literature and in this study show that it might be possible to control the formation of organo-

halogenated compounds by optimizing the electric charge. Results reported in Table 2 have been obtained in a range of operating conditions for which >98% of CBZ degradation and >70% mineralization was achieved (mass transport limitation). Therefore, it might be possible to reduce the electric charge in order to further reduce the generation of AOCl. It is also important to take into consideration that the parameter AOCl is a global indicator of the presence of such chemicals; however it does not imply any information about the nature of their toxicological effects. It is therefore also necessary to conduct more detailed studies on the formation of specific most notorious representatives of organo-halogenated compounds and the mechanisms involved in these reactions in order to determine how to really avoid or control the formation of such toxic by-products [25].

#### *3.4. Energy consumption*

Energy consumption is an important characteristic of the viability as well as a major drawback for electro-oxidation processes. Therefore, its proper analysis on a real effluent containing low concentration of pollutant was a crucial task of this study. The results are presented on fig. 5.

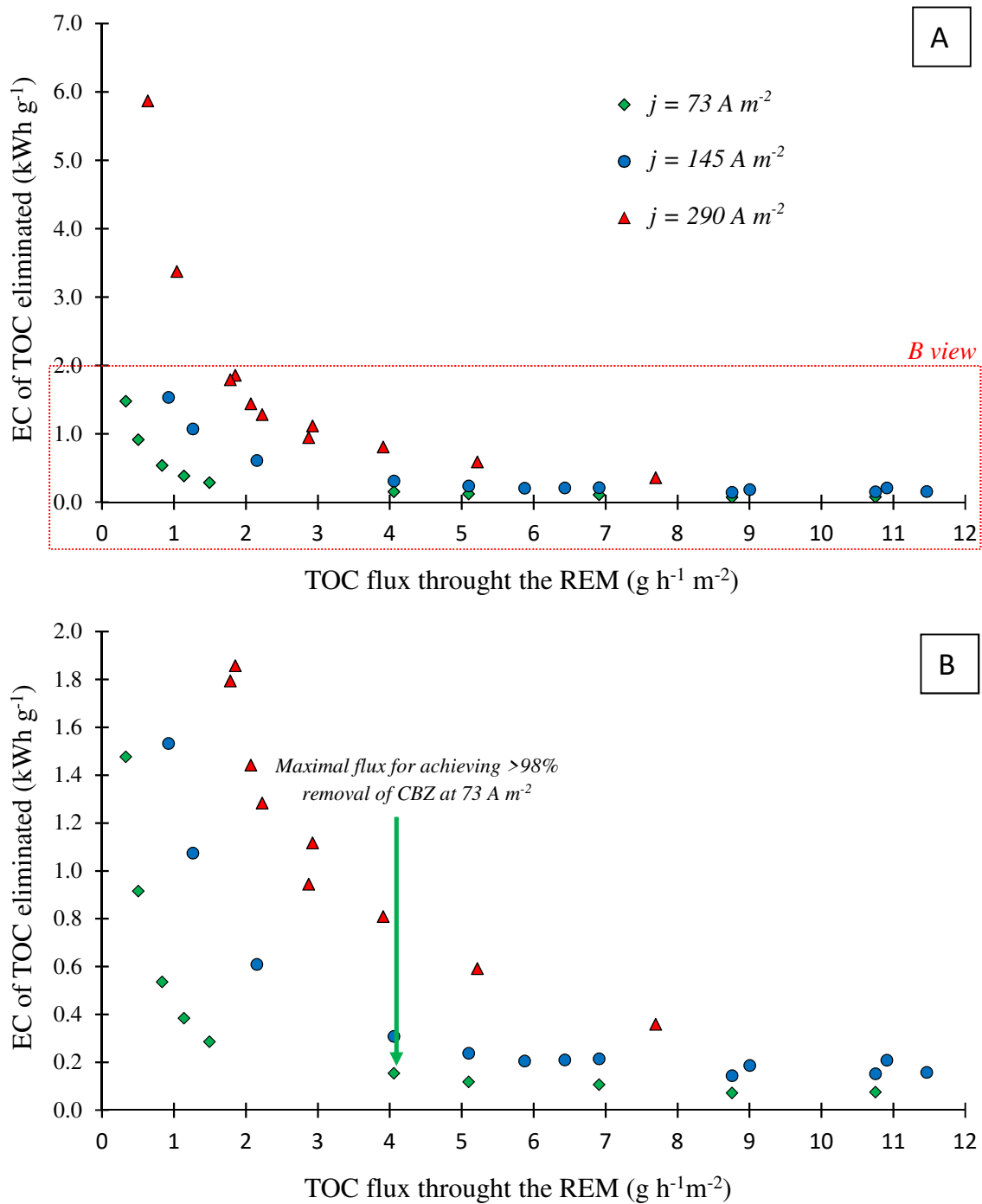


**Fig. 5.** Energy consumption per meter cube of treated water as a function of volumetric flux. A. General view B. Increased view with a smaller scale of y axe.

In fig. 5, the results of energy consumption are expressed as kWh per g of TOC eliminated and are presented as a function of TOC flux through the REM expressed in  $\text{g h}^{-1} \text{m}^{-2}$ . As expected from Eq. 1, the energy consumption initially drastically drops with the increase of the TOC flux. In fact, low energy efficiency is usually observed when operating electro-oxidation under mass transport

limitation. One of the great advantages of REM is that it is possible to improve this energy consumption by simply increasing the TOC flux through the REM. Then, at high TOC flux, when the process is operated under current limitation, the energy consumption reached a plateau around 0.1 – 0.2 kWh g<sup>-1</sup> TOC removed. As explained previously, this current limitation was reached at different TOC flux depending on the current density applied. Besides, higher energy consumption was also always observed when using the highest current densities because of the higher cell potential.

For the optimization of the process, it is crucial to take into consideration all the parameters, including the energy consumption, the removal of target compounds and the formation of by-products. For determination of the optimal parameters, it was decided to choose the current density for which the formation of AOCl and perchlorate was minimized, i.e. the lowest current density (73 A m<sup>-2</sup>). Then, the optimal TOC flux through the membrane was selected as the maximal one allowing to achieve >98% removal of CBZ, i.e. 4.1 g h<sup>-1</sup> m<sup>-2</sup> (arrow in fig. 5B). With these operating conditions, the percent of mineralization was still excellent (70%). The energy consumption was 0.15 kWh g<sup>-1</sup> TOC removed, which corresponds to 0.74 kWh m<sup>-3</sup>. This high energy efficiency of electro-oxidation for the treatment of a real effluent with low concentration is clearly related to the mass transport enhancement allowed from the use of such REM. These promising results might promote the development of this process for such applications. For comparison, the French company SUEZ is currently estimating that a reasonable cost of a tertiary treatment (for capital and operational expenditures) would be between 7 and 14 euros / population equivalent / year, including an energy consumption of 1.45 kWh m<sup>-3</sup> [39].

It is also of great interest to compare the results obtained here using Ti<sub>4</sub>O<sub>7</sub> as REM for anodic oxidation to the use of other electrochemical systems, as reported in Table 3. Recently, Yang *et al.* [40] combined the use of a BDD anode with the heterogeneous electro-Fenton process at the cathode for removal of the antibiotic ofloxacin in batch configuration. A mineralization rate of 80% was obtained after 8h of electrolysis from an effluent at 22 mgC L<sup>-1</sup>. The energy consumption was about 3.5 kWh g<sup>-1</sup> TOC (*i.e.* 77 kWh m<sup>-3</sup>). Besides, El Kateb *et al.* [29] used the same cathode material combined with plate Ti<sub>4</sub>O<sub>7</sub> anode in batch configuration for TOC abatement of the concentrate of a landfill leachate pre-treated in an MBR. An energy consumption of 0.11 kWh g<sup>-1</sup> TOC (49.5 kWh m<sup>-3</sup>)

was mentioned for TOC removal. Those high values of EC could be mainly explained by the batch configuration of the system, which is dramatically penalizing for mineralization of low concentration of pollutants because of the limitation ascribed to the diffusion of pollutants from the bulk to the electrode surface [13]. These much higher energy consumptions highlight the suitability of REM developed in this study for the treatment of low concentrations of pollutants in secondary effluents from municipal WWTP. The interest of flow-through reactors equipped with a Ti<sub>4</sub>O<sub>7</sub> REM was also confirmed by the recent paper of Le *et al.* concerning PFAS degradation [27]. The energy consumption to remove PFOA (initial concentration 4.4 mg L<sup>-1</sup>) and PFOS (initial concentration 5 mg L<sup>-1</sup>) to below the detection limit (*i.e.* 86 and 35 ng L<sup>-1</sup>) were 5.1 and 6.7 kWh m<sup>-3</sup> proving again the efficiency of Ti<sub>4</sub>O<sub>7</sub> in flow-through configuration for highly stable micropollutants.

**Table 3.** Comparison of recently published results on the degradation of organic pollutants in aqueous media by electrochemical advanced oxidation processes.

Authors	Ref.	System	Energy consumption (kWh.m <sup>-3</sup> )	Mineralization (%)	Comments
This study	-	REM TiOx	0.74	70	
SUEZ Company	39	-	1.45	-	Recommendation
Yang et al.	40	Batch BDD + Electro-Fenton	77	80 (8h)	
El Kateb et al.	29	Batch TiOx + Electro-Fenton	49.5	45 (8h)	
Lin et al.	41	Batch TiOx	14.2 – 36.9	99	
Le et al.	27	REM TiOx	5.1 – 6.7	-	

#### 4. Conclusion

The main objective of this study was to analyze the viability of the anodic oxidation process using a substoichiometric titanium oxide reactive electrochemical membrane as anode. The laboratory pilot of this coupled process was operated to treat a secondary effluent from a municipal WWTP spiked with a pharmaceutical micropollutant (CBZ) at a concentration of  $100 \mu\text{g L}^{-1}$ , which is close to an environmentally relevant value. The efficiency of this process was evaluated regarding to the removal of pollutants in terms of mineralization of the organic load as well as degradation of the micropollutant. Two major drawbacks of any electrochemical treatment processes as defined previously (toxic chlorinated by-product formation and energy consumption) were equally addressed by this study. Here are the main conclusions to draw from the results obtained.

- Mineralization and degradation demonstrated an **efficacy** above 70% removal for the low TOC flux, regardless to the current densities applied. Increasing the TOC flux revealed that the process effectiveness shifted from being limited by mass transport of pollutants to the surface of the anode to being controlled by the production of oxidant species at the anode *i.e.* by the applied current density. For each value of current density, a limiting value of TOC flux above which the effectiveness decreased was highlighted. The higher the current density, the higher this threshold value was observed.

- Formation of chlorates and perchlorates was strongly dependent on the applied current density. Increasing the current density resulted in greater formation of chlorates, while perchlorates strongly raised in their concentration for the highest current density applied. A similar trend was observed for AOX. Even low current density ( $73 \text{ A m}^{-2}$ ) led to the formation of AOX but their concentration was multiplied by 3 at high current density ( $290 \text{ A m}^{-2}$ ). The main consequence is that only the use of low current density should be considered for such applications to  $\text{Cl}^-$  containing effluents.

- It is possible to strongly decrease the energy consumption of the process by simply increasing the TOC flux in order to reduce mass transport limitations.

- Overall, by taking into consideration both advantages and drawbacks of this process, the optimal operating conditions were obtained at  $73 \text{ A m}^{-2}$  (in order to reduce the formation of toxic by-products)



and a TOC flux through the membrane of  $4.41 \text{ g h}^{-1} \text{ m}^{-2}$ , corresponding to  $1.34 \text{ m}^3 \text{ h}^{-1} \text{ m}^{-2}$ . These conditions allowed for >98% degradation of CBZ, 70% of mineralization with an energy consumption of  $0.15 \text{ kWh g}^{-1}$  of TOC removed (i.e.  $0.74 \text{ kWh m}^{-3}$  of treated wastewater). These results highlight that the development of REM based on Magnéli phases can be a cost effective electrochemical advanced oxidation process, even for the treatment of effluents with low concentrations of pollutants.

## Acknowledgements

This project is supported by Chimie Balard Cirimat Carnot Institute through the ANR program N°16 CARN 0008-01. The research group would like to thank the Carnot Institute for this financial support. We are also grateful to Dr. Jelena Radjenovich ICREA Research Professor at Catalan Institute for Water Research, Gerone, Spain and her research team for the analysis of AOX of our samples.

## References

- [1] M. Panizza, G. Cerisola, Direct and Mediated Anodic Oxidation of Organic Pollutants, *Chemical Reviews* 109(12) (2009) 6541–6569, <https://doi.org/10.1021/cr9001319>.
- [2] C. A. Martínez-Huitle, M. A. Rodrigo, I. Sires, O. Scialdone, Single and coupled electrochemical processes and reactors for the abatement of organic water pollutants: a critical review, *Chemical reviews* 115(24) (2015) 13362-13407, <https://doi.org/10.1021/acs.chemrev.5b00361>.
- [3] P. V. Nidheesh, M. Zhou, M. A. Oturan, An overview on the removal of synthetic dyes from water by electrochemical advanced oxidation processes, *Chemosphere* 197 (2018) 210-227, <https://doi.org/10.1016/j.chemosphere.2017.12.195>.
- [4] B. Marselli, J. Garcia-Gomez, P. A. Michaud, M. A. Rodrigo, C. Comninellis, Electrogenation of hydroxyl radicals on boron-doped diamond electrodes, *J. Electrochem. Soc.* 150(3) (2003) D79–D83, <https://doi.org/10.1149/1.1553790>.
- [5] Á. Anglada, A. Urriaga, I. Ortiz, D. Mantzavinos, E. Diamadopoulos, Boron-doped diamond anodic treatment of landfill leachate: evaluation of operating variables and formation of

- oxidation by-products, *Water research* 45(2) (2011) 828-838, <https://doi.org/10.1016/j.watres.2010.09.017>.
- [6] I. Moraleda, N. Oturan, C. Saez, J. Llanos, M. A. Rodrigo, M. A. Oturan, A comparison between flow-through cathode and mixed tank cells for the electro-Fenton process with conductive diamond anode, *Chemosphere* 238 (2020) 124854, <https://doi.org/10.1016/j.chemosphere.2019.124854>.
- [7] S. Garcia-Segura, J. Keller, E. Brillas, J. Radjenovic, Removal of organic contaminants from secondary effluent by anodic oxidation with a boron-doped diamond anode as tertiary treatment, *Journal of Hazardous Materials* 283 (2015) 551-557, <https://doi.org/10.1016/j.jhazmat.2014.10.003>.
- [8] E. Mousset, M. Puce, M. N. Pons, Advanced Electro-Oxidation with Boron-Doped Diamond for Acetaminophen Removal from Real Wastewater in a Microfluidic Reactor: Kinetics and Mass-Transfer Studies, *ChemElectroChem* 6(11) (2019) 2908-2916, <https://doi.org/10.1002/celec.201900182>.
- [9] B. P. Chaplin, The Prospect of Electrochemical Technologies Advancing Worldwide Water Treatment, *Accounts of Chemical Research* 52(3) (2019) 596–604, <https://doi.org/10.1021/acs.accounts.8b00611>.
- [10] L. Xu, X. Ma, J. Niu, J. Chen, C. Zhou, Removal of trace naproxen from aqueous solution using a laboratory-scale reactive flow-through membrane electrode, *Journal of Hazardous Materials*, 379 (2019) 120692, <https://doi.org/10.1016/j.jhazmat.2019.05.085>
- [11] X. Li, S. Shao, Y. Yang, Y. Mei, W. Qing, H. Guo, L. E. Peng, P. Wang, and C. Y. Tang, Engineering Interface with a One-Dimensional RuO<sub>2</sub>/TiO<sub>2</sub> Heteronanostructure in an Electrocatalytic Membrane Electrode: Toward Highly Efficient Micropollutant Decomposition, *ACS Appl. Mater. Interfaces*, 12, 19, (2020) 21596–21604, <https://doi.org/10.1021/acsami.0c02552>

- [12] M. Chen, J. Xu, R. Dai, Z. Wu, M. Liu, Z. Wang, Development of a moving-bed electrochemical membrane bioreactor to enhance removal of low-concentration antibiotic from wastewater, *Bioresource Technology*, 293 (2019) 122022  
<https://doi.org/10.1016/j.biortech.2019.122022>
- [13] C. Trellu, B. P. Chaplin, C. Coestier, R. Esmilaire, S. Cerneaux, C. Causserand, M. Cretin, Electro-oxidation of organic pollutants by reactive electrochemical membranes, *Chemosphere* 208 (2018) 159–175, <https://doi.org/10.1016/j.chemosphere.2018.05.026>.
- [14] C. Trellu, C. Coestier, J. C. Rouch, R. Esmilaire, M. Rivallin, M. Cretin, C. Causserand, Mineralization of organic pollutants by anodic oxidation using reactive electrochemical membrane synthesized from carbothermal reduction of TiO<sub>2</sub>, *Water Research* 131 (2018) 310–319, <https://doi.org/10.1016/j.watres.2017.12.070>.
- [15] E. Skolotneva, C. Trellu, M. Cretin, S. Mareev, A 2D Convection-Diffusion Model of Anodic Oxidation of Organic Compounds Mediated by Hydroxyl Radicals Using Porous Reactive Electrochemical Membrane, *Membranes* 10(5) (2020) 102-118, <https://doi.org/10.3390/membranes10050102>
- [16] F.C. Walsh, R.G.A. Wills, The continuing development of Magnéli phase titanium sub-oxides and Ebonex® electrodes, *Electrochimica Acta* 55 Issue 22 (2010) 6342-6351, <https://doi.org/10.1016/j.electacta.2010.05.011>
- [17] C. Acha, M. Monteverde, M. Núñez-Regueiro, A. Kuhn, M. A. Alario Franco, Electrical resistivity of the Ti<sub>4</sub>O<sub>7</sub> Magneli phase under high pressure. *Eur. Phys. J. B* 34, (2003) 421–  
<https://doi.org/10.1140/epjb/e2003-00240-2>
- [18] S. Andersson, B. Collén, U. Kuylenstierna, A, Phase analysis studies on the titanium-oxygen system, Magnéli, *Acta Chemica Scandinavica* 11 (1957) 1641-1652.
- [19] K. Kolbrecka, J. Przyluski, Sub-stoichiometric titanium oxides as ceramic electrodes for oxygen evolution—structural aspects of the voltammetric behaviour of Ti<sub>n</sub>O<sub>2n-1</sub>, *Electrochim. Acta*, 39(11-12) (1994) 1591-1595, [https://doi.org/10.1016/0013-4686\(94\)85140-9](https://doi.org/10.1016/0013-4686(94)85140-9).

- [20] A. Simpson, P. Carter, Method and apparatus for the manufacture of substoichiometric oxides of titanium by reduction with hydrogen, in: W. I. P. Organization (Ed.), WO 2008/037941 A1 (2008).
- [21] D. Portehault, V. Maneeratana, C. Candolfi, N. Oeschler, I. Veremchuk, Y. Grin, C. Sanchez, M. Antonietti, Facile General Route toward Tunable Magnéli Nanostructures and Their Use As Thermoelectric Metal Oxide/Carbon Nanocomposites, *ACS Nano* 5, 11, (2011) 9052-9061, <https://doi.org/10.1021/nn203265u>.
- [22] S-S. Huang, Y-H. Lin, W. Chuang, P-S. Shao, C-H. Chuang, J-F. Lee, M-L. Lu, Synthesis of High-Performance Titanium Sub-Oxides for Electrochemical Applications Using Combination of Sol-Gel and Vacuum-Carbothermic Processes, *ACS Sustainable Chem. Eng.* 6, 3 (2018) 3162–3168, <https://doi.org/10.1021/acssuschemeng.7b03189>.
- [23] L. Guo, Y. Jing, B. P. Chaplin, Development and Characterization of Ultrafiltration TiO<sub>2</sub> Magnéli Phase Reactive Electrochemical Membranes, *Environ. Sci. Technol.*, 50, 3 (2016) 1428–1436, <https://doi.org/10.1021/acs.est.5b04366>.
- [24] S. Nayak, B. P. Chaplin, Fabrication and characterization of porous, conductive, monolithic Ti<sub>4</sub>O<sub>7</sub> electrodes, *Electrochim. Acta* 263 (2018) 299-310, <https://doi.org/10.1016/j.electacta.2018.01.034>.
- [25] M. H. Lin, D. M. Bulman, C. K. Remucal, B. P. Chaplin, Chlorinated Byproduct Formation during the Electrochemical Advanced Oxidation Process at Magnéli Phase Ti<sub>4</sub>O<sub>7</sub> Electrodes, : *Environ. Sci. Technol.* 54 (2020) 12673–12683, <https://dx.doi.org/10.1021/acs.est.0c03916>.
- [26] A. M. Zaky, B. P. Chaplin, Mechanism of p-Substituted Phenol Oxidation at a Ti<sub>4</sub>O<sub>7</sub> Reactive Electrochemical Membrane, *Environ. Sci. Technol.* 48 (2014) 5857–5867, <https://dx.doi.org/10.1021/es5010472>.
- [27] T. X. H. Le, H. Haflich, A. D. Shah, B. P. Chaplin, Energy-Efficient Electrochemical Oxidation of Perfluoroalkyl Substances Using a Ti<sub>4</sub>O<sub>7</sub> Reactive Electrochemical Membrane Anode, *Environ. Sci. Technol. Lett.* 6 (2019) 504-510. <https://doi.org/10.1021/acs.estlett.9b00397>.

- [28] C. Trellu, M. Rivallin, S. Cerneaux, C. Coetsier, C. Causserand, M. A. Oturan, M. Cretin, Integration of sub-stoichiometric titanium oxide reactive electrochemical membrane as anode in the electro-Fenton process, *Chemical Engineering Journal* 400 (2020) 125936, <https://doi.org/10.1016/j.cej.2020.125936>.
- [29] M. Kateb, C. Trellu, A. Darwich, M. Rivallin, M. Bechelany, S. Nagarajan, S. Lacour, N. Bellakhal, G. Lesage, M. Héran, M. Cretin, Electrochemical advanced oxidation processes using novel electrode materials for mineralization and biodegradability enhancement of nanofiltration concentrate of landfill leachates, *Water Research* 162 (2019) 446-455, <https://doi.org/10.1016/j.watres.2019.07.005>.
- [30] J. Radjenovic, D. L. Sedlak, Challenges and Opportunities for Electrochemical Processes as Next-Generation Technologies for the Treatment of Contaminated Water. *Environmental Science & Technology*, 49(19) (2015) 11292–11302, <https://doi.org/10.1021/acs.est.5b02414>.
- [31] C. Bruguera-Casamada, I. Sirés, E. Brillas, R. M. Araujo, Effect of electrogenerated hydroxyl radicals, active chlorine and organic matter on the electrochemical inactivation of *Pseudomonas aeruginosa* using BDD and dimensionally stable anodes, *Separation and Purification Technology* 178, 2 (2017) 24–231, <https://doi.org/10.1016/j.seppur.2017.01.042>
- [32] M. H. Bergmann, J. Rollin, T. Iourtchouk, The occurrence of perchlorate during drinking water electrolysis using BDD anodes, *Electrochimica Acta* 54(7) (2009) 2102-2107, <https://doi.org/10.1016/j.electacta.2008.09.040>.
- [33] A. Sánchez-Carretero, C. Sáez, P. Cañizares, M. A. Rodrigo, Electrochemical production of perchlorates using conductive diamond electrolyses, *Chemical Engineering Journal* 166(2) (2011) 710-714, <https://doi.org/10.1016/j.cej.2010.11.037>.
- [34] A. Donaghue, B. P. Chaplin, Effect of select organic compounds on perchlorate formation at boron-doped diamond film anodes, *Environmental science & technology* 47(21) (2013) 12391-12399, <https://doi.org/10.1021/es4031672>.
- [35] E. Emmanuel, G. Keck, J.-M. Blanchard, P. Vermande, Y. Perrodin, Toxicological effects of disinfections using sodium hypochlorite on aquatic organisms and its contribution to AOX

- formation in hospital wastewater. *Environment International* 30(7) (2004) 891–900, <https://doi.org/https://doi.org/10.1016/j.envint.2004.02.004>.
- [36] C. Grøn, Organic Halogen Group Parameters as Indicators of Ground Water Contamination, *Groundwater Monitoring & Remediation*, 13(3) (1993) 148–158, <https://doi.org/10.1111/j.1745-6592.1993.tb00084.x>
- [37] Y. Xie, L. Chen, R. Liu, AOX contamination status and genotoxicity of AOX-bearing pharmaceutical wastewater. *Journal of Environmental Sciences*, 52 (2017) 170–177, <https://doi.org/https://doi.org/10.1016/j.jes.2016.04.014>.
- [38] V. Schmalz, T. Dittmar, D. Haaken, E. Worch, Electrochemical disinfection of biologically treated wastewater from small treatment systems by using boron-doped diamond (BDD) electrodes—Contribution for direct reuse of domestic wastewater. *Water Research* 43(20) 5 (2009) 260–5266, <https://doi.org/10.1016/j.watres.2009.08.036>.
- [39] Ywann Penru, Journée de restitution des résultats du projet Micropolis, in: 2018
- [40] W. Yang, M. Zhou, N. Oturan, M. Bechelany, M. Cretin, M. A. Oturan, Highly efficient and stable FeII/FeIII LDH carbon felt cathode for removal of pharmaceutical ofloxacin at neutral pH, *Journal of Hazardous Materials* 393 (2020) 122513, <https://doi.org/10.1016/j.jhazmat.2020.122513>.
- [41] H. Lin, J. Niu, S. Liang, C. Wang, Y. Wang, F. Jin, Q. Luo, Q. Huang, Development of macroporous Magnéli phase  $Ti_4O_7$  ceramic materials: As an efficient anode for mineralization of poly- and perfluoroalkyl substances, *Chemical Engineering Journal* 354 (2018) 1058–1067, <https://doi.org/10.1016/j.cej.2018.07.210>.